Understanding Dark Matter using Galactic Rotation Curves

A B. Tech Project Report Submitted
in Partial Fulfillment of the Requirements
for the Degree of

Bachelor of Technology

by

Ashwani Rajan
(150121008)

under the guidance of

Dr. Sovan Chakraborty

Dr. Sayan Chakrabarti

to the

DEPARTMENT OF PHYSICS

INDIAN INSTITUTE OF TECHNOLOGY GUWAHATI
GUWAHATI - 781039, ASSAM

CERTIFICATE

*This is to certify that the work contained in this thesis entitled "**Understanding Dark Matter using Galactic Rotation Curves**" is a bonafide work of **Ashwani Rajan** (**Roll No. 150121008**), carried out in the Department of Physics, Indian Institute of Technology Guwahati under my supervision and that it has not been submitted elsewhere for a degree.*

Supervisors: **Dr. Sovan Chakraborty**

Dr. Sayan Chakrabarti

Assistant Professors,

Department of Physics,

Indian Institute of Technology Guwahati, Assam.

22nd April 2019

Guwahati.

Abstract

Dark matter plays an important role in explaining different astronomical and cosmological phenomena. Understanding and explaining the dark matter distribution around galaxies is a field focussed by a good fraction of the literature on extra galactic astronomy and cosmology.In this work, we focus on understanding the galactic rotation curve and the role of Dark Matter in explaining the Rotation curves. We perform a detailed analysis of the Galactic Rotation Curve of the Milky Way galaxy using a non-truncating self consistent Isothermal model of Dark Matter Halo and numerically generate the rotation curves for this model. Then we attempt to improve this model by including different types of truncation profiles for this standard model. As the next step, we attempt to explain the observed galactic rotational velocity data by including a Yukawa-like correction term to the newtonian potential obtained due to our standard model. We then analyse the Rotation curves obtained by different cases of density distributions which arise by selecting different sets of galactic components. We tune the fit parameters to give the best fits for each of these cases using maximum likelihood estimation algorithm and compare the fit probability value for each case in order to find the Density distribution profile which best explains the observed rotational velocity data.

Contents

1 Introduction

1.1 Historical Background

The question of what makes up the mass density of the universe is as old as extragalactic astronomy which began with the recognition that nebulae such as M31 in Andromeda are actually galaxies like our own. In **1933**, **Zwicky** derived the velocity dispersion of some of the galaxies in **Coma Cluster** from the Doppler shifts of the spectral lines of these galaxies, and hence could estimate the cluster mass. He concluded that the Coma cluster contained far more mass than luminous matter when he translated the luminosity of the galaxies into a corresponding mass. In **1939**, **Babcock** measured the mass distribution of M31. From the measurement of radial velocities in the optical emission line region extending to 20 kpc from the center of M31, **Babcock determined that the total mass-to-light ratio increases in the outer regions**. He suggested that absorption of light was the reason of this increasing mass-to-light ratio. Since then evidences have supported the fact that the mass density associated with luminous matter cannot explain the observed dynamics on such galactic scales.

Eventually in the 1970s, it had become clear that dark matter was an unavoidable part of the universe composition and by mid 1980s the concept that the universe is dominated by an unknown form of matter or by an unfamiliar class of dark astronomical objects became quite the reality among scientists.

1.2 Evidences of Dark Matter

A wide variety of evidence has accumulated in support of dark matter's existence. In **1932**, **Jan Hendrik Oort** analysed the vertical motion of all known stars near the Galactic plane and used this data to calculate the acceleration of matter. Contradictory to the expectations, the calculated potential provided by the known stars was not sufficient to keep the stars bound to the Galactic disk. According to Oort, since the Galaxy was stable, there had to be some "missing matter" near the Galactic plane exerting gravitational attraction. This was the first indication for the possible presence of dark matter in our Galaxy.

Other evidences at galactic scales include **galactic rotation curves**, the weak **gravitational lensing** of distant galaxies by foreground structures and the weak modulation of strong lensing around large elliptical galaxies. The **velocity dispersions** of stars in some dwarf galaxies imply that they contain as much as 10^3 times more mass than what can be estimated from their luminosity. On the scale of galaxy clusters, observations indicate a total cosmological matter density of $\Omega_M \approx 0.2\neg 0.3$, which is much larger than the corresponding density in baryons. It was these measurements of velocity dispersions in the Coma cluster which led Fritz Zwicky to believe that large quantities of non-luminous matter should be present. On cosmological scales, observations of the **anisotropies in the Cosmic Microwave Background** have lead to an estimation of the total matter density of $\Omega_M h^2 = 0.1326 \pm 0.0063$, where h is the Hubble parameter in units of 100 km/sec per Mpc. In contrast, this information combined with measurements of the light chemical element abundances leads to an estimate of the baryonic density given by $\Omega_B h^2 = 0.02273 \pm 0.00062$.

Other notable evidence is the **X-ray emitting galactic groups** formed by a small number of galaxies which are enveloped in a large cloud of hot gas (ICM). The total amount of baryonic matter can be estimated by adding the amount of matter in the form of hot gas deduced from the intensity of this radiation to the observed luminous matter. In clusters studied, the gas fraction increases with the distance from the center; which indicates the presence of dark matter. Taken together, these observations strongly lead us to the conclusion that 80-85% of the matter in the universe by mass consists of non-luminous and non-baryonic material.

In this project, we study the Galactic Rotation Curves of spiral galaxies. We generate the galactic rotation curves of milky way generated using a non-truncated isothermal model of the dark matter halo along with density distribution of visible matter described by a spheroidal bulge superposed on an axisymmetric disk. The rest of the report is arranged as follows: Section 2 elaborates on Galactic Rotation Curves of spiral galaxies and how they serve as a strong evidence of the presence of Dark Matter Halos as a part of the galactic mass distribution. In Section 3, we descirbe our model of the Dark Halo as well as the visible matter of the galaxy. We also explain our process of generating the galactic rotation curves by solving Poisson equation

for the density distributions of Dark matter halo and visible matter. Section 4 includes the Rotation Curve and Density Profile for non-truncating Self-consistent Isothermal Halo Model. We then attempt to improve our previous model in Section 5 by including three different types of truncations in our previous model. In Section 6, we explore the possibility including Yukawa-like correction term to our isothermal SHM density distribution as well as to the NFW profile. Section 7 shows the calculaton procedure for the Rotation Curves. Then we use Maximum likelihood estimation procedure to find the best fit parameters to fit our suggested rotational curves to observational data. Finally, we present our results in Section 9 and 10, which includes the rotation curves for different cases of density distribution taken into consideration. We conclude all the aspects of our work in section 11.

2 Galactic Rotation Curves

Spiral galaxies are stable gravitationally bound systems where the visible matter is composed of stars and interstellar gas. Most of the visible matter is in a relatively thin disc, where stars and gas rotate around the galactic center on nearly circular orbits. **The rotation curve of a spiral galaxy is a plot of the orbital rotation speed of visible stars or gas in that galaxy versus their radial distance from the galaxy's centre**. To plot a rotation curve, we calculate the rotational velocity of objects such as stars at different radial distances of a galaxy by measuring their Doppler shifts, and then plot this quantity versus their respective distance away from the center.

If the circular velocity at radius r is v in a galaxy with mass *M(r)* inside r, the condition for stability is that the **centrifugal acceleration** $\frac{v}{r}$ should equal the **gravitational pull** $\frac{GM(r)}{r^2}$, and the radial dependence of v would then be expected to follow **Kepler's law**.

$$v = \sqrt{(G\frac{M(r)}{r})}$$

From figure 1, we can see the shape the rotation curve should have. However, the actual observed curve is roughly flat as r increases outside of the core region.

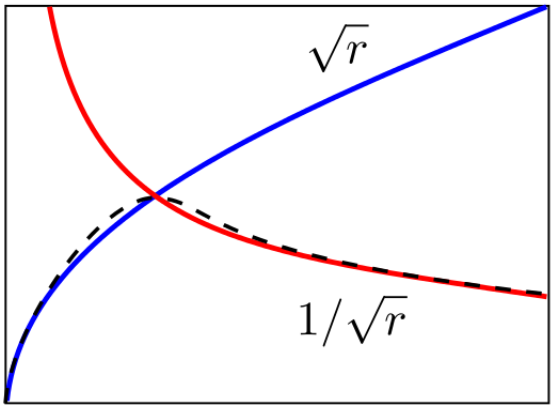

Figure 1: Expected galactic Rotation curve

Results from measurements of galactic rotation curves show that the velocity does not follow this $\frac{1}{\sqrt{r}}$ law, but stays constant after attaining a maximum at about 5 kpc. The most approachable solution to this can be that the visible part of the galaxies are fitted in large extending halos of dark matter. If the enclosed mass inside the radius r, *M(r)*, is proportional to r it follows that $v(r) \approx constant$.

A flat rotation curve is one in which the velocity is constant over some range of radii which implies that the mass is still increasing linearly with radius. Most galaxies have rotation curves that show solid body rotation in the very center, following by a slowly rising or constant velocity rotation in the outer parts.

Notably, the rotation curves of most galaxies can be fitted by the superposition of stellar and gaseous disks, both represented by mass extending in thin disk with sometimes a bulge at the center and the dark halo, modeled by an isothermal sphere. Thus there are a lot of possible models depending on the relative contributions of visible matter disk and dark matter.

Figure 2: measured rotation curve of **NGC6503** with best fit and contributions from halo, disk and gas.

Figure 2 is the measured rotation curve of **NGC6503** with best fit and contributions from halo, disk and gas. We can note that that at very small

radii the dark halo component is indeed much smaller than the luminous disk component. At large radii, however, the need for a halo of dark matter can be obviously concluded from the plot.

On galactic scales, the contribution of dark matter generally dominates the total mass. Note the contribution of the baryonic component, negligible for small masses but increasingly important in the larger structures.

Our Galaxy is complicated because of a density dip at 9 kpc and a smaller

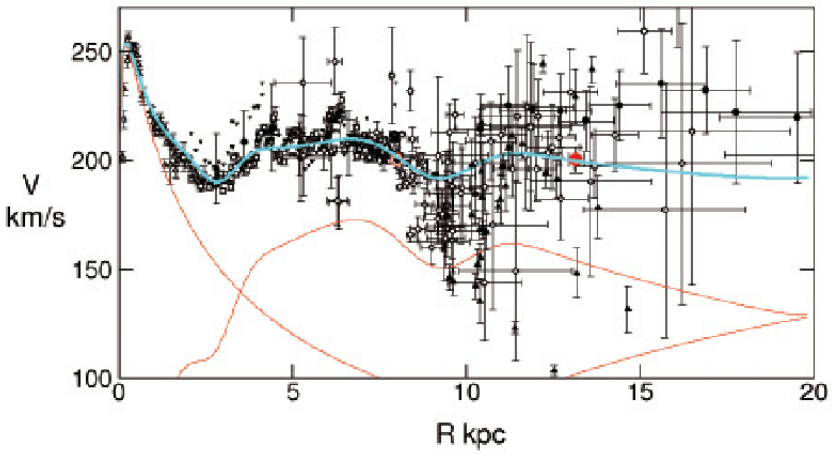

Figure 3: the rotation curve of the Milky Way with contributions from the central bulge, stellar disk + interstellar gas and dark matter halo (the red curves from left to right)

dip at 3 kpc, as is seen in Figure 3. To fit the measured rotation curve, we require at least three contributing components: a central bulge, the star disk + gas, and a dark matter halo. For small radii there is a choice of empirical rotation curves, and no dark matter component appears to be needed until radii beyond 15 kpc.

3 Calculations

3.1 Self-consistent Isothermal Model of Dark Matter Halo

Starting with the particle model, **Weakly Interacting Massive Particles**(WIMPs) are the candidates for the Dark Matter used in our analysis. Their masses typically lies in the range of a few GeV to a few TeV. Such particles are predicted in many models of physics beyond the standard model of particle physics.

Because of their weak interactions, these particles are expected to "freeze out" in the early Universe at a temperature scale of MeV, and would be present in the Universe today as 'cold' dark matter with an estimable abundance that can naturally explain the measured cosmological density of dark matter in the Universe. Also, the measured rotation curves of spiral galaxies can be explained naturally under the hypothesis that the visible galaxies are embedded in much larger, and roughly spherical dark matter "halos". The true extents and the masses of such halos are, however, unknown.

The DM halo of the Galaxy is assumed to be described by a **single component isothermal sphere** with a **Maxwellian velocity distribution** in the Galactic rest frame given by

$$f(\mathbf{x},\mathbf{v})d^3\mathbf{v} = 4\pi\rho(\mathbf{x})[\tfrac{3}{2\pi<v>^2}]^{\frac{3}{2}} exp[-\tfrac{3v^2}{2<v>^2}]dv$$

Here $v = |\mathbf{v}|$, $\rho(\mathbf{x})$ is the density at the location $\mathbf{x}$, and $< v^2 >^{\frac{1}{2}}$ is the velocity dispersion.Evolution of systems of collisionless particles like WIMPs under the process of gravitational collapse is governed by the process of "violent relaxation" suggested by Lynden-Bell whereby the observationally relevant 'coarse-grained' phase space distribution function (DF) of the system rapidly relaxes, due to collective effects, to a quasi-Maxwellian stationary state which is a steady-state solution of the collision-less Boltzmann equation.

The value of the velocity dispersion, $< v^2 >^{\frac{1}{2}}$, the single parameter that characterizes the Maxwellian velocity distribution of the DM $< v^2 >^{\frac{1}{2}} = \sqrt{\frac{3}{2}} v_{c,\infty}$ particles, is usually determined from the relation between the velocity dispersion of the particles constituting a single-component self-gravitating

isothermal sphere and the asymptotic value of the circular rotation speed, $v_{c,\infty}$ of a test particle in the gravitational field of the isothermal sphere. Assuming $v_{c,\infty} = v_{c,\odot} \approx 220kms1$, we can calculate $v_{c,\infty} \approx 270$ km/s.

This isothermal non-truncating sphere model of the DM halo with a value of the DM velocity dispersion $< v^2 >^{\frac{1}{2}} \approx 270$ km/s and local value of the DM density $\rho_{DM,\odot} \approx 0.3$ GeV/cm is what is often referred to as the **Standard Halo Model**(SHM). We are considering the halo to abide to the principles of SHM hereafter.

3.2 Numerical Solution to generate Rotation Curves

The Maxwellian velocity distribution following the SHM model is related to the phase-space Distribution Function of the isothermal sphere, which extends infinitely with a divergent total mass, and is characterized by two parameters, σ and ρ_0.

$$f_{IS}(\mathbf{x}, \mathbf{v}) = \frac{\rho_0}{(2\pi\sigma^2)^{\frac{3}{2}}} exp[\frac{-E}{\sigma^2}]$$

Here $3\sigma^2 =< v^2 >$ and E is the total energy per unit mass of the halo, given by $E = \Phi(x) + \frac{1}{2}v^2$. $\Phi(x)$ being the total gravitational potential with the boundary condition $\Phi(0) = 0$.

Hence the density at any point x is given by:

$$\rho_{IS}(\mathbf{x}) = \rho_0 exp[\frac{-\Phi(x)}{\sigma^2}]$$

We assume that the density distribution of the visible matter can be effectively described by the well-known model of a spheroidal bulge superposed on an axisymmetric disk. The density distributions of these components are given by

$$\rho_s(r) = \rho_s(0)(1 + \frac{r^2}{a^2})^{-\frac{3}{2}}$$

$$\rho_d(r) = \frac{\Sigma_\odot}{2h} e^{-\frac{(R-R_0)}{R_d}} e^{-\frac{|z|}{h}}$$

where $r = (R^2 + z^2)^{\frac{1}{2}}$. Generally considered values for the parameters are $\rho_s(0) = 4.2 \times 10^2 M_\odot pc^{-3}$, $a = 0.103$ kpc , $R_d = 3$ kpc, and $h = 0.3$ kpc, with $R_0 = 8.5$ kpc, the solar Galactocentric distance, and $\Sigma_\odot \approx 48 M_\odot pc^{-2}$, the surface density of the disk at the solar location.

The expressions for the gravitational potentials, ϕ_s and ϕ_d, corresponding to above forms of ρ_s and ρ_d can be directly calculated analytically or by using our numerical Poisson solver. Hence, we can calculate $\phi_{vis} = \phi_s + \phi_d$.

Thus, we should write $\Phi(x) = \Phi_{DM}(x) + \Phi_{vis}(x)$

where now $\Phi_{DM}(x)$ represents the contribution of the DM component to the total gravitational potential in presence of the visible matter, and $\Phi_{vis}(x)$ is the gravitational potential of the observed visible matter of the Galaxy.

We can write their respective Poisson equations as follows:

$$\bigtriangledown^2 \Phi_{DM}(x) = 4\pi G \rho_{DM}(x)$$

$$\bigtriangledown^2 \Phi_{vis}(x) = 4\pi G \rho_{vis}(x)$$

We can solve for the potential of dark matter by solving the Poisson Equation for ρ_{DM} and Φ_{DM} using **"iterative numerical methods"**. We used **"4th order Runge-kutta method"** to iteratively calculate the values of Φ_{DM} at frequent intervals of r.

The visible matter distribution ρ_{vis} (and hence the potential Φ_{vis}) is known from various observational data and modeling therefore solutions of Poisson Equation can be calculated with appropriate boundary conditions, which is chosen as :

$$(\bigtriangledown \Phi_{vis})_{|x|=0} = (\bigtriangledown \Phi_{DM})_{|x|=0} = 0$$

$$\Phi_{vis}(0) = \Phi_{DM}(0) = 0$$

These give us a two-parameter family of solutions for $\Phi_{DM}(x)$ and $\Phi_{vis}(x)$ for chosen values of the parameters (ρ_0, σ).

For a particular solution, the rotation curve of the Galaxy, $v_c R$, i.e., the circular rotation velocities in the equatorial plane of the Galaxy as a function of the Galactocentric distance (**R**) on the equatorial plane, can be calculated from:

$$v_c(R) = R\frac{\delta}{\delta R}[\Phi_{total}(R, z = 0)] = R\frac{\delta}{\delta R}[\Phi_{vis}(R, z = 0) + \Phi_{DM}(R, z = 0)]$$

z being the distance normal to the equatorial plane. The best-fit values of the two parameters can then be determined by comparing the theoretically calculated rotation curves with the observed data on the rotation curve of the Galaxy.

4 Rotation Curve and Density Profile for Non-Truncating Self-consistent Isothermal Halo Model

Using the above equation for $v_c(R)$, We generated the galactic rotation curve for the milky way galaxy. According to the Standard Halo Model which we are using, and from $3\sigma^2 =< v^2 > \sigma$ was calculated to be approximately equal to 464 km/sec. Similarly, we used the value of $\rho_0 \approx 0.3$ Gev/cm^3 which is in agreement with Standard Halo Model. The plot is illustrated in figure 4.

Similarly, we generated the plot for the density distribution of the Dark Matter halo with respect to distance. Since our Standard Halo Model was non -truncating, we expect the plot to be a nearly straight line which decays to $\rho_{DM,z=0} = 0$ as $R \to \infty$. The density distribution attains values around $\rho_{DM,z=0} = 0.4$ Gev/cm^3, which is as assumed according to SHM. The plot is shown in figure 5.

5 Truncating the Dark Matter Halo Density Distribution

The Standard Halo model(SHM) was found to be a sufficient model for the initial calculation of Dark matter halo velocity distribution. However, a

major drawback of the SHM was lack of a proper truncation on the density distribution. Hence, in order to further improve the model, we attempted a couple of updates in the Standard Halo model so as to include a truncation on the density distribution of the halo. The importance of such a truncation can be emphasised by the fact that the isothermal sphere model has a mass that linearly increases with its radius r and tends to ∞ as $r \to \infty$. Such a system cannot represent a realistic Dark Matter halo of finite physical size. This truncation attempt would help make the SHM Density distribution closer to realistic and contribute in a more accurate derivation on velocity distribution for the Halo.

Our naive approach was to include a straight-forward truncation radius(r_t) such that the dark matter density distribution vanishes at $r > r_t$. Hence the Hence the density at any point x is given by:

$$\rho_{IS}(\mathbf{r}) = \begin{cases} \rho_0 exp[\frac{-\Phi(\mathbf{r})}{\sigma^2}], & r \leq r_t. \\ 0, & r > r_t. \end{cases} \tag{1}$$

It can be seen that the density of Dark Matter abruptly drops to zero after the truncation radius(r_t) which leads to abnormal behaviour at the boundary of the Halo and a larger drop in the gravitational potential due to dark matter halo than expected the effect of which can be seen in the velocity distribution plot(Figure (7).). Taking truncation radius(r_t) = $100kpc$ and plotting the velocity distribution using the equation

$$v_{DM}(R) = R\frac{\delta}{\delta R}[\Phi_{DM}(R, z = 0)] \tag{2}$$

Where $\Phi_{DM}(R, z = 0)$ can be calculated numerically using the Poisson's Equation.

$$\bigtriangledown^2 \Phi_{DM}(x) = 4\pi G \rho_{DM}(x) \tag{3}$$

It can be noted that although the dark matter density drops to zero at the truncation radius(r_t), yet the dark matter potential is gradually declining to zero after truncation radius and hence so is the velocity distribution. The velocity distribution here implies that for any particle trapped beyond $r > r_t$, it would have a velocity which declines depending on the distance from the galactic center.

The next approach was to include an exponentially decreasing density distribution for $r > r_t$ so as to remove an abrupt decrease in density after a truncation radius and replace it with a gradual decline in Halo density as

shown in Figure (6). The density distribution was modified as follows and the graphically shown in Figure (6).

$$\rho_{IS}(\mathbf{r}) = \begin{cases} \rho_0 exp[\frac{-\Phi(\mathbf{r})}{\sigma^2}], & r \leq r_t. \\ \rho(r_t) exp[\frac{-(r-r_t)}{r_s}], & r > r_t. \end{cases} \tag{4}$$

Here, we use truncation radius as the distance from where the gradual decline in the density distribution starts. We use an extra parameter, scale radius(r_s) which is introduced as a scale factor for the density distribuion. Scale radius plays a role in deciding the extent to which the dark matter halo density is spread, i.e. increasing the scale radius increases the spread for dark matter and decreasing the scale factor decreases the same. We have used scale radius($r_s \approx 230$) here according to the extention of Milky way Halo. The velocity distribution for the same can be seen in Figure (7). We find that there is still an abrupt change in velocity at truncation radius due to the change in density distribution functions at $r = r_t$. We can see that in case of this distribution, the velocity has a less steeper decline rate than the previous density profile since the Halo density is finite beyond truncation radius as well, which contributes to the velocity of Halo particles at disatances beyond truncation radius.

However, what we expect is not an abrupt change in density but a smoother change right from the galactic center in order to make it more realistic. Also ,it can be seen that the velocity distribution increases exponentially at $r \leq r_t$ as a result of the above density distributions which should not be the case for a realistic model. Hence in order to make the distribution continuous and further more realistic, we have multiplied an exponentially decreasing term to the entire density distribution. Here again, we have used the scale radius parameter (r_s) in order to tune the extent of spread and it was observed that as scale radius increases, the spread as well as mass under Dark Matter distribution increases. For our purpose, we have taken the scale radius to be $r_s \approx 230kpc$ as that is approximately the distance to which the dark matter halo of Milky Way extends. As a result, we see a smooth velocity distribution which first increases to around $150kmsec^{-1}$ and then gradually drops at higher radii.

$$\rho_{IS}(\mathbf{r}) = \rho_0 exp[\frac{-\Phi(\mathbf{r})}{\sigma^2}] exp[\frac{-r}{r_t}] \tag{5}$$

6 The Yukawa Correction

The Yukawa-like corrections to traditional Newtonian potential are generally of the form

$$\Phi(\mathbf{x}) = -G \int \frac{\rho(\mathbf{x}')}{|\mathbf{x}-\mathbf{x}'|} \left(1 + \beta e^{-|\mathbf{x}-\mathbf{x}'|/\lambda}\right) d^3\mathbf{x}' \ . \tag{6}$$

We get the term for Newtonian gravity when $\beta = 0$, or at scales of $|\mathbf{x}-\mathbf{x}'| >> \lambda$. In the case of $|\mathbf{x}-\mathbf{x}'| << \lambda$, gravitational force could be stronger or weaker then the newtonian term depending on the sign of β.

We considered the Navarro-Frenk-White profile (hereafter NFW), a spherical distribution for dark matter halo obtained from N-body simulations of cold dark matter (CDM),

$$\rho_{\rm NFW}(r) = \frac{\rho_s}{\frac{r}{r_s}(1+\frac{r}{r_s})^2} \ , \tag{7}$$

where ρ_s is the characteristic density and r_s is the scale radius.These terms are related by the concentration parameter $c \equiv r_{200}/r_s$ and $M_{200} \equiv (4\pi/3)200\rho_{\rm crit} r_{200}^3$, where $\rho_{\rm crit}$ is the critical density, M_{200} is the critical mass of the Halo and r_{200} is the critical radius. Therefore, we can express the NFW profile with respect to a single parameter, i.e. M_{200}. Hence, we can find the relation between $(\rho_s, r_s) \to (c, M_{200})$ as follows:

$$\rho_s = \frac{200}{3} \frac{c^3 \rho_{\rm crit}}{\ln(1+c) - \frac{c}{1+c}} \ , \tag{8}$$

$$r_s = \frac{1}{c} \left(\frac{3M_{200}}{4\pi 200 \rho_{\rm crit}}\right)^{1/3} \tag{9}$$

For halos of size ≈ 100 kpc and larger, we can write the $c - M_{200}$ relation:

$$c(M_{200}) = 10^{0.905} \left(\frac{M_{200}}{10^{12} h^{-1} \mathrm{M}_\odot}\right)^{-0.101} \ . \tag{10}$$

Hence, the equation (9) can be written as

$$r_s \approx 28.8 \left(\frac{M_{200}}{10^{12} h^{-1} \mathrm{M}_\odot}\right)^{0.43} \mathrm{kpc} \ , \tag{11}$$

where $\rho_{\rm crit} = 143.84\ \mathrm{M}_\odot/\mathrm{kpc}^3$ and $h = 0.671$.

We can find the expression for the gravitational potential by inserting the equation (7) in the equation (6). The potential Φ comes out to be a sum of the Newtonian potential for a NFW profile, $\Phi_{\rm NFW}$, with the additional term, the modified gravity part $\Phi_{\rm mg}(r)$. Solving Poisson's equation for gives the gravitational potential $\rho_{\rm NFW}(r)$ and $\Phi_{\rm mg}(r)$ to be

$$\Phi_{\rm NFW}(r) = -\frac{4\pi G\rho_0 r_s^3}{r}\ln\left(1+\frac{r}{r_s}\right) \tag{12}$$

with the limits $\lim_{r\to\infty}\Phi_{\rm NFW}(r) = 0$ and $\lim_{r\to 0}\Phi_{\rm NFW}(r) = -4\pi G\rho_0 r_s^2$

$$\Phi_{\rm mg}(r) = \frac{2\pi G\beta\rho_s r_s^3}{r}\Bigg\{\exp\left(-\frac{r_s+r}{\lambda}\right)\left[{\rm Ei}\left(\frac{r_s}{\lambda}\right) - {\rm Ei}\left(\frac{r_s+r}{\lambda}\right)\right] + \\ -\exp\left(\frac{r_s+r}{\lambda}\right){\rm Ei}\left(-\frac{r_s+r}{\lambda}\right) + \exp\left(\frac{r_s-r}{\lambda}\right){\rm Ei}\left(-\frac{r_s}{\lambda}\right)\Bigg\}\,, \tag{13}$$

where ${\rm Ei}(x)$ is the error function variation defined as

$${\rm Ei}(x) = -\int_{-x}^{\infty}\frac{e^{-t}}{t}dt\,, \tag{14}$$

Here, three parameters, i.e. $(\beta, \lambda, M_{200})$ play a decisive role in fitting the galaxy rotation curves to the observational data. M_{200} is a galaxy-specific parameter and $M_{200} \approx 6.41 \pm 4.1 \times 10^{11} M_\odot$ for the Milky Way galaxy Ref.(2). The parameter β measures the strength of the 'fifth-force' interaction while the second parameter, λ, gives its range.

7 Rotational Velocity Calculation

As we have previously done in the first part of this project, we evaluate the kinematics of Milky Way galaxy considering the components to be analysed being: the elongated disk component, the spherical bulge at center and the dark matter halo. The total circular velocity at the galactic plane, V_c is related to the total gravitational potential, Ψ as follows:

$$V_c^2 = r\frac{d\Psi}{dr}\,. \tag{15}$$

We assume that the potential responsible for the acceleration for baryonic components is the Newtonian, while the potential responsible for dark matter is given by equation (6), i.e the Yukawa corrections on NFW profile. Thus, the total gravitational potential can be written as

$$\Psi = \Phi_{\rm disk} + \Phi_{\rm bulge} + \Phi_{\rm NFW} + \Phi_{\rm mg} \ . \tag{16}$$

Due to the linear nature of equation (15), we can split the total circular velocity into of each different component.

$$V_c^2(r) = V_{\rm disk}^2(r) + V_{\rm bulge}^2(r) + V_{\rm NFW}^2(r) + V_{\rm mg}^2(r) \ , \tag{17}$$

We have calculated the velocity components due to Circular Disk and Spherical Bulge in our previous calculations using their respective density distributions as:

$$\rho_s(r) = \rho_s(0)(1 + \frac{r^2}{a^2})^{-\frac{3}{2}} \tag{18}$$

$$\rho_d(r) = \frac{\Sigma_\odot}{2h} e^{-\frac{(R-R_0)}{R_d}} e^{-\frac{|z|}{h}} \tag{19}$$

where $r = (R^2 + z^2)^{\frac{1}{2}}$. Generally considered values for the parameters are $\rho_s(0) = 4.2 \times 10^2 M_\odot pc^{-3}$, $a = 0.103$ kpc , $R_d = 3$ kpc, and $h = 0.3$ kpc, with $R_0 = 8.5$ kpc, the solar Galactocentric distance, and $\Sigma_\odot \approx 48 M_\odot pc^{-2}$, the surface density of the disk at the solar location. The corresponding potentials can be calculated analytically using Poisson's equations.

We can use equation (15) to directly calculate $V_{\rm NFW}^2(r)$ and $V_{\rm mg}^2(r)$ from $\Phi_{\rm NFW}$ and $\Phi_{\rm mg}$ respectively. The components $V_{\rm NFW}$ and $V_{\rm mg}$ are given by:

$$V_{\rm NFW}^2(r) = \frac{4\pi G r_s^3 \rho_s}{r} \left[-\frac{r}{r + r_s} + \ln\left(1 + \frac{r}{r_s}\right) \right] \tag{20}$$

$$V_{\rm mg}^2(r) = -\frac{2\pi G \beta \rho_s r_s^3}{r} \Bigg\{ \frac{2r}{r_s + r} + \exp\left(\frac{r_s + r}{\lambda}\right) \left(\frac{r}{r_s} - 1\right) \mathrm{Ei}\left(-\frac{r_s + r}{\lambda}\right) + \exp\left(-\frac{r_s + r}{\lambda}\right) + \\ + \exp\left(-\frac{r_s + r}{\lambda}\right) \left(1 + \frac{r}{\lambda}\right) \left[\exp\left(\frac{2r_s}{\lambda}\right) \mathrm{Ei}\left(-\frac{r_s}{\lambda}\right) + \mathrm{Ei}\left(\frac{r_s}{\lambda}\right) - \mathrm{Ei}\left(\frac{r + r_s}{\lambda}\right) \right] \Bigg\} \tag{21}$$

8 Maximum Likelihood Estimation of Parameters

Next, we find the best-fit values for the free parameters, which are $\{\beta, \lambda\}$, against the observational data. We assumed here that the errors of the observed rotation curve data follow a Gaussian distribution, so that we can build the likelihood for Milky Way galaxy as follows

$$\mathcal{L}(\beta, \lambda) = \prod_{i=1}^{N} \frac{1}{\sqrt{2\pi}\sigma_i} \exp\left\{ -\frac{1}{2}\left(\frac{V_{\rm obs}(r_i) - V_c(r_i, \beta, \lambda)}{\sigma_i} \right)^2 \right\} \tag{22}$$

$$\mathcal{L}(\beta, \lambda) = (2\pi)^{-N/2} \left\{ \prod_{i=1}^{N} \sigma_i^{-1} \right\} \exp\left\{ -\frac{1}{2} \sum_{i=1}^{N} \left(\frac{V_{\rm obs}(r_i) - V_c(r_i, \beta, \lambda)}{\sigma_i} \right)^2 \right\} \tag{23}$$

Considering log Likelihood in order to ease the calculations, we get

$$\mathbf{L}(\beta, \lambda) = -\frac{N}{2} \log 2\pi - \sum_{i=1}^{N} \log \sigma_i - \frac{1}{2} \sum_{i=1}^{N} \left(\frac{V_{\rm obs}(r_i) - V_c(r_i, \beta, \lambda)}{\sigma_i} \right)^2 \tag{24}$$

where N is the number of observational points for each galaxy, σ_i is the data error, $V_{\rm obs}(r_i)$ is the observed circular velocity of the Milky Way galaxy at the radius r_i and $V_c(r_i, \beta, \lambda)$ is the total rotation curve, which was expressed in equation (17).

8.1 Observatonal Data

We use the values of $V_{\rm obs}(r_i)$ as provided by P. Bhattacharjee et al (2014). They constructed the Milky Way Rotation Curve starting from its very inner regions (few hundred pc) out to a large galactocentric distance of approximately 200 kpc using kinematical data on a variety of tracer objects moving in the gravitational potential of the Galaxy, without assuming any theoretical models of the visible and dark matter components of the Galaxy. They have compiled the data in such a way that the effect on the RC due to the uncertainties in the values of the Galactic Constants (GCs) R_0 and V_0 (these being the sun's distance from and circular rotation speed around the Galactic center, respectively) are taken to be constant for the observational data to be

consistent throughout. We have used the data compiled by them in order to perform Maximum Likelihood Estimation to fit the parameters. For (β, λ) to be the best fit, the log likelihood function has to be maximum. Such value of (β, λ) can be found by equating the partial derivatives of the log likelihood function to zero and calculating (β, λ) values from these equations.

$$\frac{\delta \mathbf{L}(\beta, \lambda)}{\delta \beta} = 0 \tag{25}$$

$$\frac{\delta \mathbf{L}(\beta, \lambda)}{\delta \lambda} = 0 \tag{26}$$

We have taken into consideration different cases for Milky way's Galactic Roataion Curve from Equation (17) by selecting some components at a time and four different cases arise which are discussed in next section.

9 Improved Galactic Rotation Curves

We plot the Galactic Rotation Curves for a few different cases using the equation (17). We select different components each time to plot them along with the observed Rotation Curve data points in order to compare the fits obtained from the pair of equations (25, 26).

9.1 NFW Density Distribution Profile for Dark Matter

First, we only consider the NFW profile from equation (7) for the Dark Matter density distribution along with the Spherical Bulge and Circular disk distribution for visible matter. In this case, the Total Circular velocity V_c is given by :

$$V_{c1}^2(r) = V_{\text{disk}}^2(r) + V_{\text{bulge}}^2(r) + V_{\text{NFW}}^2(r) \tag{27}$$

We plotted the above equation with respect to r in Figure (8). It can be seen that the NFW profile does not add up much as an independent dark matter profile by itself. This leads to the gradual decrease in the Rotational Curve at larger r from galactic center. The Kolmogorov–Smirnov test (K-S test) gives a p-value that the observed points are derived from the given profile $V_{c1}^2(r)$ is $P = 0.426$. This implements that the null hypothesis can be rejected

Table 1: The circular velocity, V_c, and its 1-σ error, Δ, for various values of the Galactocentric distance, r, for a radial profile of the non-disk tracers with $[R_0(kpc), V_0(kms^{-1})] = [8.3, 244]$.

r (kpc)	V_c $(kmps)$	ΔV_c $(kmps)$	r (kpc)	V_c $(kmps)$	ΔV_c $(kmps)$
0.20	233.0	13.32	38.41	191.57	11.73
0.38	268.92	4.67	40.42	197.59	14.12
0.66	250.75	11.35	42.40	192.79	5.92
1.61	217.83	5.81	44.49	213.22	17.17
2.57	219.58	1.48	45.99	179.39	11.23
3.59	223.11	2.43	48.06	213.03	24.72
4.51	247.88	2.99	49.49	178.57	17.63
5.53	253.14	1.69	51.39	183.31	23.58
6.50	270.95	2.19	53.89	157.89	19.57
7.56	267.80	0.96	56.89	191.76	24.35
8.34	270.52	0.66	57.98	210.72	29.81
9.45	235.58	8.44	60.92	168.02	25.67
10.50	249.72	13.44	64.73	206.47	36.27
11.44	261.96	11.71	69.31	203.62	40.89
12.51	284.30	17.50	72.96	190.53	40.98
13.53	271.54	15.57	76.95	222.72	74.37
14.59	251.43	25.60	81.13	186.29	66.53
16.05	320.70	25.27	84.90	122.25	36.46
18.64	286.46	101.18	89.35	143.95	29.49
26.30	189.64	6.74	92.44	154.66	67.23
28.26	237.99	11.54	97.41	184.0	72.86
29.51	209.82	9.16	100.72	108.68	40.99
32.04	179.14	6.65	106.77	137.15	53.17
33.99	170.37	6.93	119.98	150.18	25.46
36.49	175.92	6.62	189.49	125.01	37.32

with a probability of 42.6% i.e. The above profile $V_{c1}^2(r)$ is able to explain the observational dat 42.6% of the times.

9.2 NFW and Modified Gravity Density Distribution Profile for Dark Matter

Next we consider both the modified gravity profile and the NFW Dark Matter density distribution profile along with the Spherical Bulge and Circular disk distribution for visible matter. The Total Circular velocity V_{c2} is given by :

$$V_{c2}^2(r) = V_{\text{disk}}^2(r) + V_{\text{bulge}}^2(r) + V_{\text{NFW}}^2(r) + V_{\text{mg}}^2(r) \tag{28}$$

The plot is shown in Figure (9). It can be seen from the plot that due to addition of an extra modified gravity potential profile, we have obtained higher values at $r > 50kpc$ from the galactic center. The p-value obtained from KS test is $p = 0.638$. This p-value is obtained at $(\beta, \lambda) = (0.1, 100)$ from MLE and it can be concluded that $V_{c2}^2(r)$ profile is a better fit to the observational data than $V_{c1}^2(r)$

9.3 SHM Isothermal Sphere Density Distribution Profile for Dark Matter

For the next case, we consider our previous work on the Self-consistent Isothermal Standard Halo Model of Dark Matter which we used for generating rotational curves. We combine this model with the Modified gravity term obtained from NFW profile along with the visible matter profiles given by circular disk and spherical bulge. This results in a plot given by:

$$V_{c3}^2(r) = V_{\text{disk}}^2(r) + V_{\text{bulge}}^2(r) + V_{\text{SHM}}^2(r) + V_{\text{mg}}^2(r) \tag{29}$$

It can be seen from Figure (10) that this profile is comparatively a worse fit to the observational data since the SHM Dark matter profile is low at r close to the galactic center. Hence, the values estimated at the range $(0 < r < 20kpc)$ are lower than the observed values. This profile also overestimates the values at $r > 60kpc$, hence the total circular velocity plot is overestimated at that range. As expected, the KS test returns a p-value of 0.326 which reflects the low fit for $(\beta, \lambda) \approx (0.2, 110)$.
In order to make the Dark Matter profile fit better on the observational data, we attempted to use the third truncation profile to our Dark matter given by Equation (5). This truncation was chosen because of its continuous nature and its similarity to realistics mass distribution systems. The new total circular velocity is given by:

$$V_{c3}^2(r) = V_{\text{disk}}^2(r) + V_{\text{bulge}}^2(r) + V_{\text{Truncated SHM}}^2(r) + V_{\text{mg}}^2(r) \tag{30}$$

In this case, we find the best fit parameters (β, λ) to be approximately (0.1, 100) and the generated galactic roataion curve was found to have a better fit to the observational data at the range of $r > 50kpc$. However, it can be observed from Figure (11) that our Rotation curve is not a good fit at smaller galactocentric distances. The p-value as a result of KS test was found to be $P = 0.413$ which is a better fit than the non-truncated case for SHM Dark matter model.

9.4 Modified Gravity Model for Dark Matter excluding other Density Models

Next we skip both the dark matter profiles and look at the rotational curves formed by just the circular disk, the spherical bulge and the modified gravity profiles due to the NFW profile. This results in a plot given by:

$$V_{c4}^2(r) = V_{\text{disk}}^2(r) + V_{\text{bulge}}^2(r) + V_{\text{mg}}^2(r) \tag{31}$$

In this case, since we just have the modified gravity profile and no dark matter profile, we do not expect a good fit for the observational data. However, on calculating (β, λ) from Maximum Likelihood estimation, we find the values of $(\beta, \lambda) \approx (0.43, 520)$ for a good fit. Using these (β, λ) values, we find p-value for ks-test to be $P = 0.638$. However, on looking at Figure (12) it can be easily noticed that the fit for $V_{c4}^2(r)$ at $r > 50kpc$ is not as good as in the range $0 < r < 30kpc$. This results from the adjustment of (β, λ) values to be such that the overall fit for total circular velocity is good. In that process, the fit at $r > 50kpc$, i.e the Dark matter dominant region is compromised. Since the value of λ and β is comparatively large in this case, we can explain the expansion in the Modified gravity profile in the plot.

10 Results

We generated the Galactic Rotation curves for milky way numerically considering the non-truncating self consistent isothermal model of dark matter halo and its density distribution(Figures 4 and 5). Next, we attempt to include three diffferent types of truncations in the standard model and plot the density distributions and numerically calculate the rotational velocity distribution for the new models(Figures 6 and 7). Finally, we have obtained the Galactic Rotation curves for five different cases which arise on selecting

different sets of galactic components.(Figures 8, 9, 11, 10 and 12). We then attempt to calculate the best fit parameters (β, λ) for each of these cases and compare the fit probability value using KS test. These values can be found in table 2.

Table 2: Best Fit parameters (β, λ) and the fit probability values for different density distribution profiles.(SB: Spherical Bulge, CD: Circular Disk, NFW: Navarro–Frenk–White profile, MG: Modified Gravity Profile, SHM: Standard Halo Model)

Density profile components	(β, λ)	P-value(P)
CD + SB + NFW	–	0.426
CD + SB + NFW + MG	(0.1,100)	0.638
CD + SB + Non-truncating SHM + MG	(0.2,110)	0.326
CD + SB + Truncating SHM + MG	(0.1,100)	0.413
CD + SB + MG	(0.43,520)	0.638

11 Conclusion

Dark matter is an essential ingredient in a good fraction of the literature on extra galactic astronomy and cosmology. Since dark matter cannot be made of any of the usual standard-model particles, dark matter is also a central focus of particle physics.

In the initial part of the project, our aim was to generate the galactic rotation curves of spiral galaxies given the density distribution of all the components (visible matter + dark matter halo) of the galaxy. Assuming the dark matter halo to be a single-component self-gravitating non-truncating isothermal sphere following the SHM model and assuming the density distribution of the visible matter described by the well-known model of a spheroidal bulge superposed on an axisymmetric disk, we were able to generate the Galactic Rotation Curve of the Milky Way, by solving the Poisson equation for the above density distributions.

Next, we improve the previous SHM halo Density distribution profile by including three different types of truncations to the initial density distribution. Paramenters (r_t, r_s) were included to implement such truncations, where r_t was the truncation radius which is used to tune the radius after which the density profile starts declining and r_s is the scale radius, used to tune the extent to which the Dark Matter halo extends from galactic center. The Truncated density distribution 2 (Equation 4) was found to be closely represent the SHM Dark matter Density distribution given by other models as well. So it was considered for later studies. Next, we added the Yukawa-like correction terms obtained from NFW profile to our different galactic density distribution profiles and fitted for the Yukawa error term parameters (β, λ) to the observational data using Maximum likelihood estimation. We looked at four different cases of Density distribution and in each case we found the best fit parameters (β, λ). It was observed that the best fit was observed for profiles which included (a) Spherical bulge, Circular disk, Dark matter NFW profile and Modified Gravity profile i.e $V_{c2}^2(r)$(Equation (28)), and (b) Spherical bulge, Circular disk and modified gravity profile i.e $V_{c4}^2(r)$(Equation (30)). The p-values were obtained to be $P = 0.638$ in both cases. However, on a closer look at both the Rotation curves makes it clear that $V_{c4}^2(r)$(Equation (30)) is merely giving a good fit because it fits better at the range of $r < 30kpc$ and not because it fits better for the dark matter dominant region. From the fact that $V_{c3}^2(r)$(Equation (29)) does not give a good fit, compared to $V_{c2}^2(r)$(Equation (28)), it can be concluded that the dark matter particles move with a larger circular velocity at small galactocentric distances and then gradually undergo a decline in circular velocity as we move away from the galactic center.

References

[1] Soumini Chaudhurya, Pijushpani Bhattacharjee, Ramanath Cowsik, *Direct detection of WIMPs : Implications of a self-consistent truncated isothermal model of the Milky Way's dark matter halo.* `https://arxiv.org/pdf/1006.5588v2.pdf`

[2] Pijushpani Bhattacharjee, Soumini Chaudhury, Susmita Kundu *ROTATION CURVE OF THE MILKY WAY OUT TO 200 KPC.* `https://arxiv.org/pdf/1310.2659.pdf`

[3] Álefe de Almeida, Luca Amendola, Viviana Niro *Galaxy rotation curves in modified gravity models*. https://arxiv.org/pdf/1805.11067.pdf

[4] Matts Roos, *Dark Matter: The evidence from astronomy, astrophysics and cosmology*. https://arxiv.org/pdf/1001.0316v2.pdf

[5] Guido D'Amico, Marc Kamionkowski, Kris Sigurdson, *Dark Matter Astrophysics*. https://arxiv.org/pdf/0907.1912v1.pdf

[6] Louis E. Strigari, *Galactic Searches for Dark Matter*. https://arxiv.org/pdf/1211.7090v1.pdf

[7] Dan Hooper, *TASI 2008 Lectures on Dark Matter*. https://arxiv.org/pdf/0901.4090v1.pdf

[8] G.G. Raffelt, *Dark Matter: Motivation, candidates and searches*. https://xxx.lanl.gov/pdf/hep-ph/9712538v1

[9] Salvatore Capozziello, Mariafelicia De Laurentis, *The dark matter problem from f (R) gravity viewpoint*. https://onlinelibrary.wiley.com/doi/pdf/10.1002/andp.201200109

[10] Christian G. Bohmer, Tiberiu Harko, Francisco S. N. Lobo, *Dark matter as a geometric effect in f(R) gravity*. https://arxiv.org/pdf/0709.0046.pdf

[11] Valery Rashkov, Annalisa Pillepich, Alis J. Deason, Piero Madau, Constance M. Rockosi, Javiera Guedes and Lucio Mayer *A "LIGHT," CENTRALLY CONCENTRATED MILKY WAY HALO?*. https://iopscience.iop.org/article/10.1088/2041-8205/773/2/L32/meta

[12] Julio F. Navarro, Carlos S. Frenk, Simon D.M. White *The Structure of Cold Dark Matter Halos*. https://arxiv.org/pdf/astro-ph/9508025.pdf

[13] Ethem Alpaydin *Introduction to Machine Learning*.

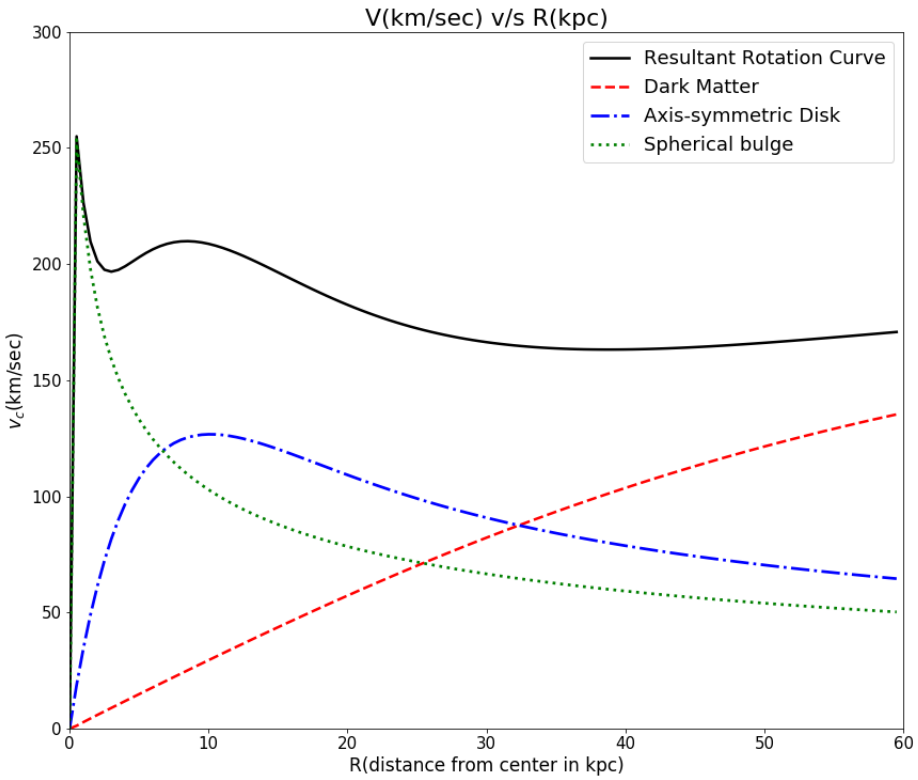

Figure 4: Numerically generated rotation curve of the Milky Way with contributions from the spheroidal bulge, stellar disk + interstellar gas and dark matter halo

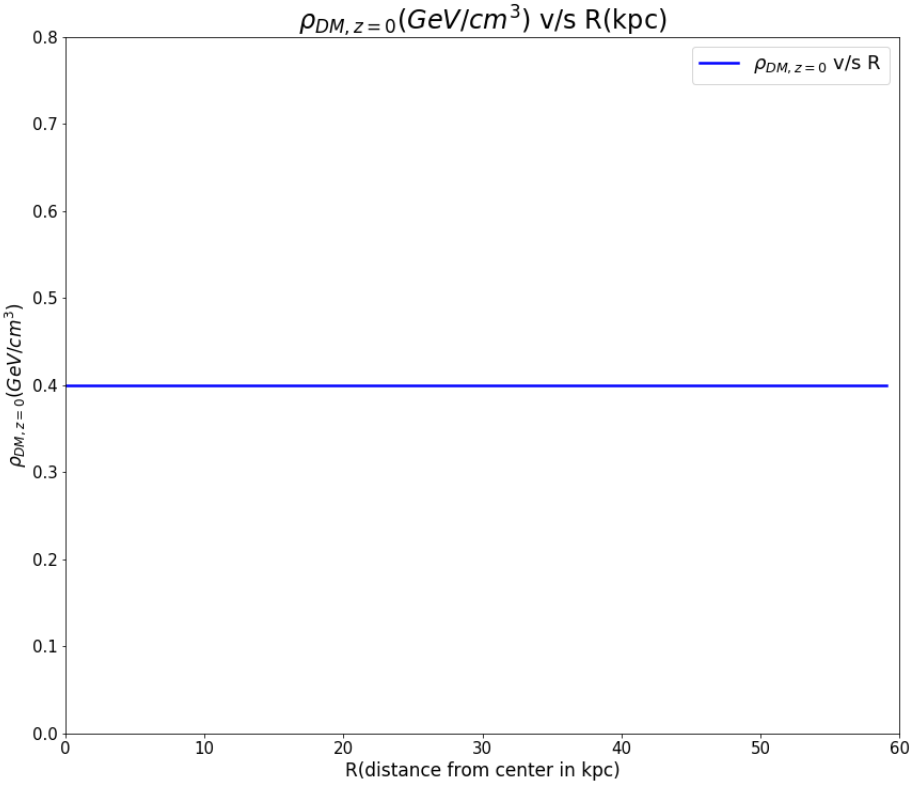

Figure 5: Numerically generated curve for $\rho_{DM,z=0}$ v/s Radial Distance for the Milky Way. Due to the non-truncating nature of our model used, $\rho_{DM,z=0}$ diminishes to zero anly at $R \to \infty$

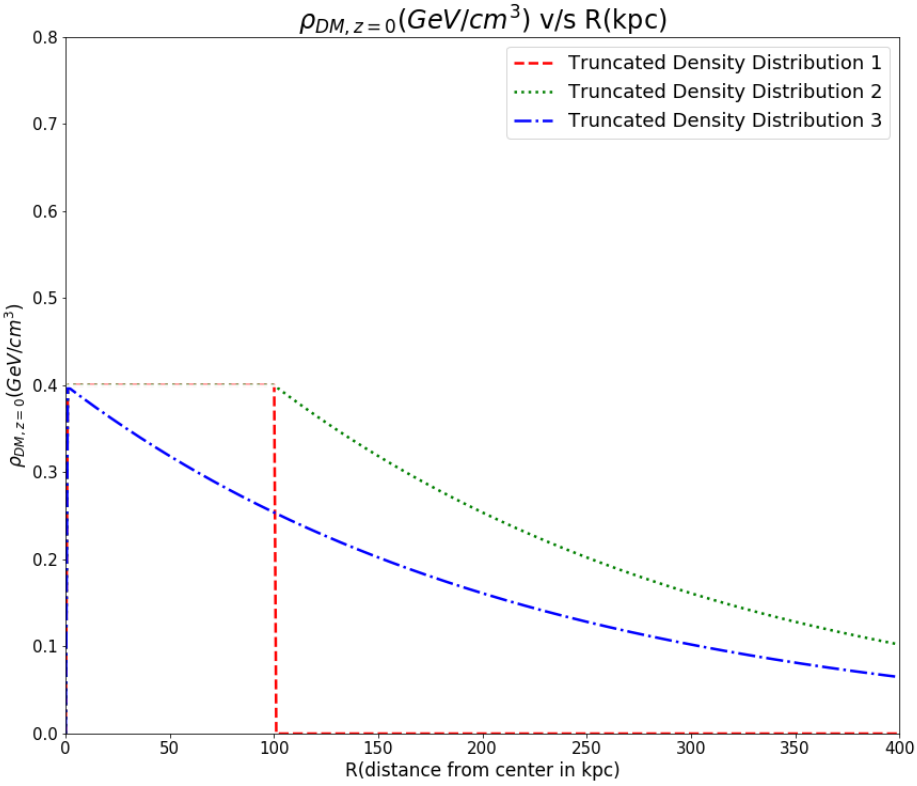

Figure 6: The truncated density distribution profiles obtained as a result of Eq. 1, 2 and 3 applied on the SHM density distribution of the Milky way Dark Matter Halo. In all cases, $r_t = 100kpc$ and $r_s = 230kpc$.

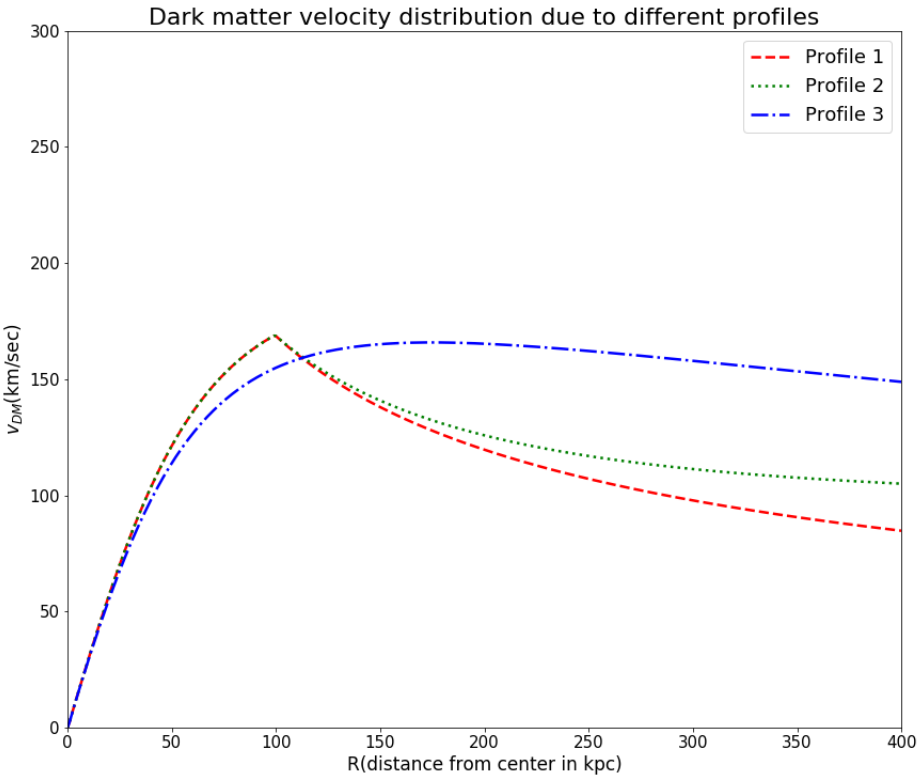

Figure 7: The velocity distribution curves for the Dark matter Halo of Milky way obtained as a result of truncations(Eq. 1, 2 and 3) applied on the SHM density distribution.

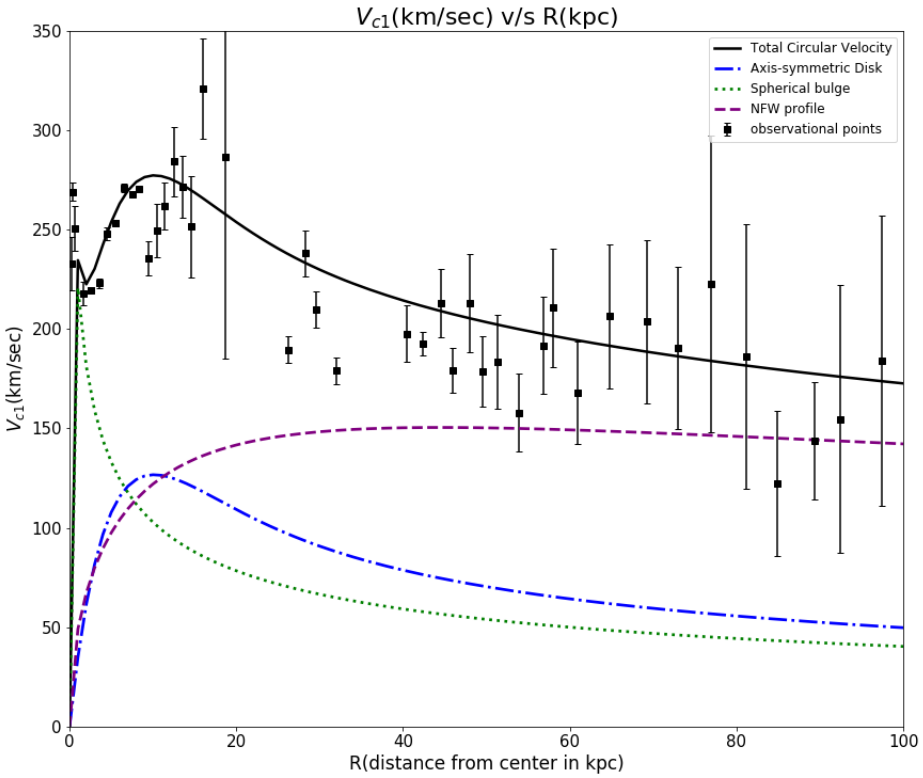

Figure 8: The Galactic Rotation Curve obtained for NFW Density Distribution Profile for Dark Matter Halo.(Equation 27)

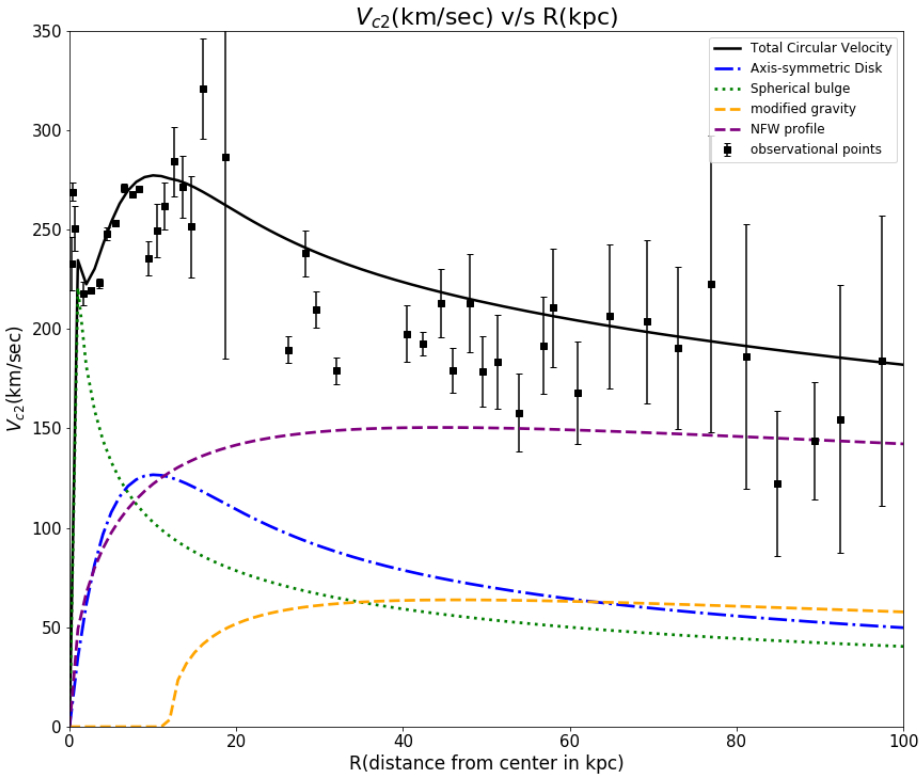

Figure 9: The Galactic Rotation Curve obtained for NFW and Modified Gravity Density DistributionProfile for Dark Matter(Equation 28)

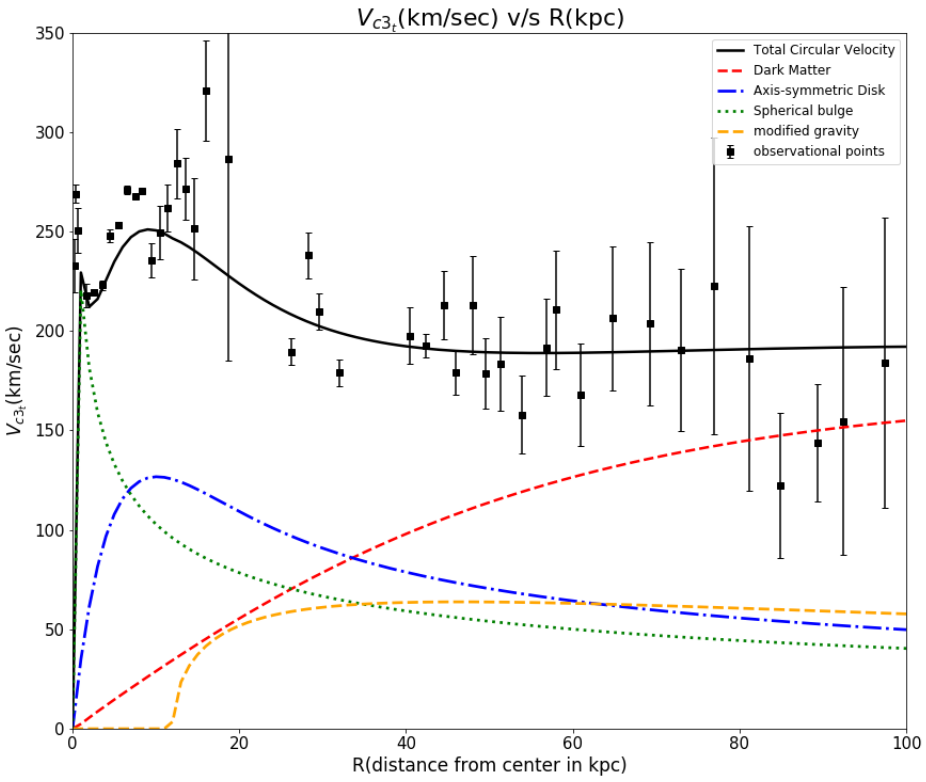

Figure 10: The Galactic Rotation Curve obtained for non- truncated SHM Isothermal Sphere Density Distribution Profile for Dark Matter(Equation 29)

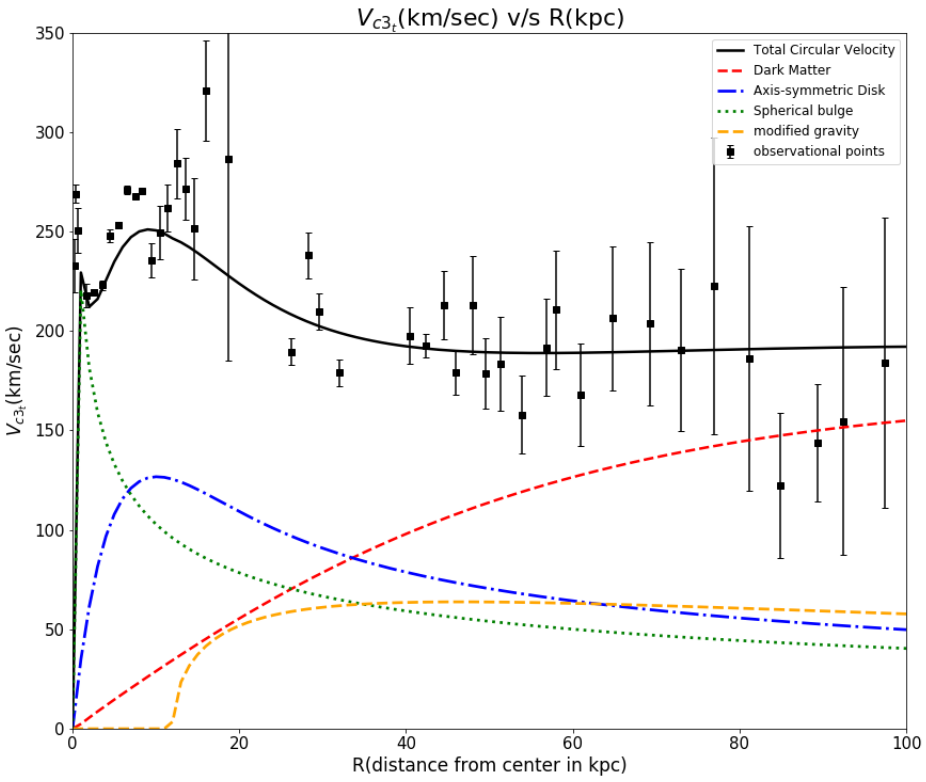

Figure 11: The Galactic Rotation Curve obtained for truncated SHM Isothermal Sphere Density Distribution Profile for Dark Matter(Equation 30)

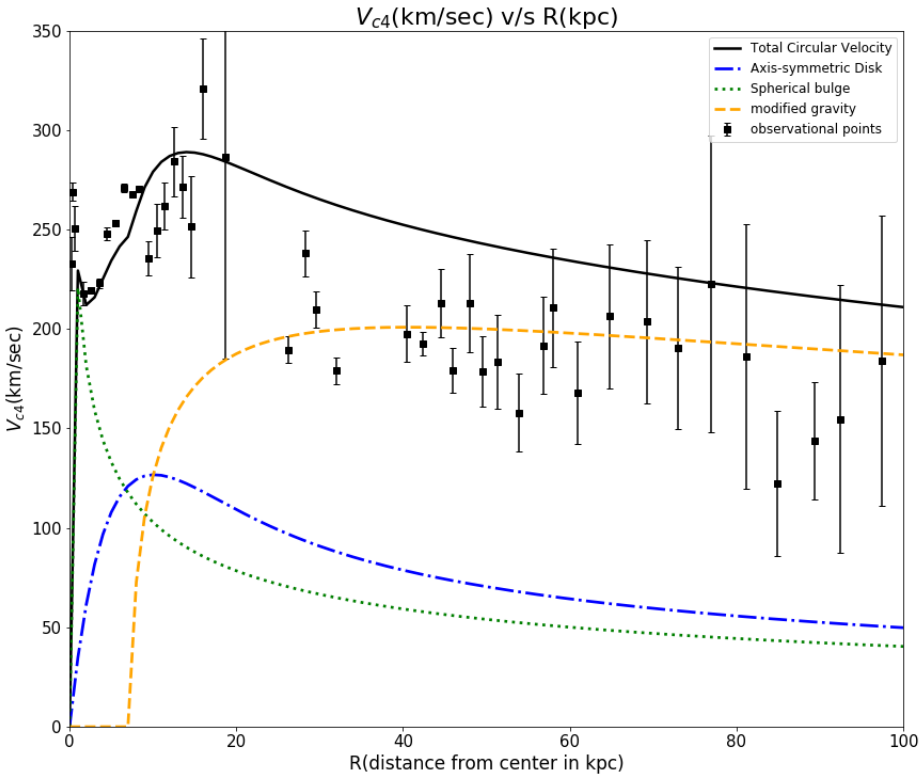

Figure 12: The Galactic Rotation Curve obtained for Modified Gravity Model for Dark Matter excluding other Density Models(Equation 31)